EFFECT OF PLASMA NITRIDING PARAMETERS
ON THE WEAR RESISTANCE OF ALLOY INCONEL 718

Halim Kovací,[1] Hojjat Ghahramanzadeh ASL,[1] Çigdem Albayrak,[2] Akgün Alsaran,[1] and Ayhan Çelik[1]

The effect of the temperature and duration of plasma nitriding on the microstructure and friction and wear parameters of Inconel 718 nickel alloy is investigated. The process of plasma nitriding is conducted in a nitrogen-hydrogen gaseous mixture at a temperature of 400, 500 and 600°C for 1 and 4 h. The modulus of elasticity of the nitrided layer, the micro- and nanohardness, the surface roughness, the friction factor and the wear resistance of the alloy are determined prior to and after the nitriding. The optimum nitriding regime providing the best tribological characteristics is determined.

Key words: Inconel 718, plasma nitriding, sliding, wear, friction.

INTRODUCTION

Refractory nickel alloy Inconel 718 is used in turbine blades, power generation, petroleum refining and nuclear reactors due to its high mechanical properties at moderate and high temperatures [1 – 5]. The alloy possesses high corrosion and oxidation resistances [2], but its wear resistance is not satisfactory [6, 7]. To widen the ranges of application of this alloy and prolong the service life articles fabricated from it, it is subjected to different kinds of surface treatment [6]. One of such methods is plasma nitriding [8], which yields a hard surface layer and a diffusion zone.

Plasma nitriding is used to raise the resistance of alloys based on ferrous and nonferrous metals to wear, fatigue and corrosion [9, 10]. Many authors have studied plasma nitriding as a method for improving the surface properties of nickel alloys. Plasma nitriding applied to Inconel 625 in [11] increased the surface hardness of the alloy by about a factor of 4.5. In [12], three layers were detected on the surface of Inconel 690 depending on the reactivity of the nitrogen-containing plasma. In [13], formation of a surface CrN layer after plasma nitriding at 560°C promoted growth in the corrosion resistance of alloy Inconel 625. The authors of [14] studied the surface layer in Inconel 600 varying the duration and the temperature of the plasma nitriding process (within 1 – 40 h and 400 – 600°C, respectively). The thickness of the

layer decreased upon growth of the temperature above the critical level of 450°C. In [15], similar results were obtained in plasma nitriding of a nickel-base dental alloy (wirolloy). In contrast to the data of [14], the thickness of the CrN layer in [16] increased continuously upon growth in the duration and the temperature of the plasma nitriding.

It should be noted that plasma nitriding of alloy Inconel 718 has been studied little. In [17, 18] plasma nitriding of Inconel 718 yielded a layer of CrN and simultaneously lowered the friction factor. The authors of [6] conducted the nitriding process of Inconel 718 with intensification of plasma below 500°C. After this treatment, the wear and corrosion resistances of the alloy were substantially higher than in the untreated specimens.

Different opinions on the mechanism of wear of Inconel 718 can be found in [6, 17, 18]. By the data of [17, 18] the average specific rate of wear grows after plasma nitriding despite lowering of the friction factor. On the contrary, the authors of [6] presume that the specific rate of wear of the alloy after plasma nitriding has not been computed appropriately due to the effects of polishing and adhesive wear. Analysis of published data shows that it is necessary to study the structure and the mechanical behavior of Inconel-type alloys after plasma nitriding conducted and different temperatures for different times. This has become the aim of the present work.

METHODS OF STUDY

We studied alloy Inconel 718 of the following chemical composition (in wt.%): 0.08 C, 55.0 Ni, 21.0 Cr, 3.30 Mo,

---

[1] Atatürk University, Engineering Faculty, Department of Mechanical Engineering.
[2] Erzincan University, Refahiye College of Vocational Studies.

5.50 Nb, 1.15 Ti, 1.00 Co, 0.35 Mn, 0.35 Si, 0.80 Al, 0.30 Cu, the remainder Fe.

The surface of initial specimens $15 \times 11 \times 1$ mm in size was polished against an emery paper with 1200-mesh grit and alumina powder with particle size 3 μm. Then the specimens were washed with ethyl alcohol and placed into a chamber for plasma nitriding; to clean the surface form contaminants it was subjected to hydrogen sputtering for 15 min at a voltage of 500 V and a pressure in the chamber 5×10^2 Pa. Plasma nitriding was conducted at DC voltage and a pressure of 5×10^2 Pa.

The specimens were treated in a nitrogen-hydrogen mixture $H_2 : N_2 = 1 : 1$ at 400, 500 and 600°C for 1 and 4 h. Accordingly, we denoted the specimens 400-1, 400-4, etc. When the process was finished, the specimens were cooled in vacuum for 6 h. The x-ray phase analysis was performed with the help of a Rigaku diffractometer in copper K_α radiation at 30 kV and 30 mA. The structure of the nitrided specimens was studied under a JEOL 6400 scanning electron microscope. The microhardness $HV_{0.01}$ was measured using a STRUERS ODURAMIN 5 device at a load of 0.1 N (10 g) with a hold of 10 sec under the load. The nanohardness and the elastic modulus were determined by the method of nanoindentation using an IBIS Nanoindentation system. The tribological studies were conducted at a temperature of 20 ± 2°C and relative air humidity of 50 ± 5% in a Turkyus pin-on-disc device. The sliding path under a load of 5 N was 150 m in 3000 sec; the rider was a ball from tungsten carbide 6 mm in diameter. The width of the wear tracks was 8 mm for all the specimens. To compute the wear rate, the profiles of the wear tracks and the surface roughness were measured by a Mahr M1 profilometer. The wear rate v_w (mm^3/N · m) was computed from the relation

$$v_w = W/(w\,s),$$

where W is the decrease in the volume, w is the normal load, and s is the sliding path. In addition, the worn surfaces were studied under a ZEISS EVO SEM scanning electron microscope.

RESULTS AND DISCUSSION

The x-ray diffraction patterns of untreated and plasma nitrided specimens of alloy Inconel 718 are presented in Fig. 1. The diffraction patterns of the specimens in the initial (untreated) condition bear the lines corresponding to the phase composition of the alloy. Plasma nitriding yields CrN nitride. Since the nitride layer is thin, the diffraction patterns of the nitrided specimens contain peaks of the substrate. The main part of chromium reacts with nitrogen and forms the nitride. In addition, the reflections from the base metal become less intense and broaden. This is explainable by changes in the composition and formation of a nitride layer on the surface. The formation of this hard layer with higher
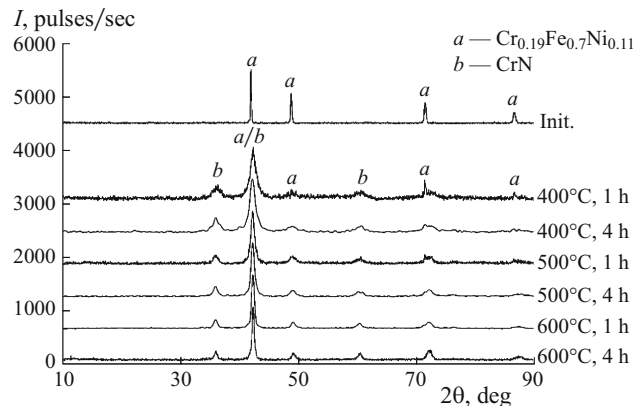

Fig. 1. X-ray diffraction patterns of alloy Inconel 718 prior to and after plasma nitriding at 400, 500 and 600°C for 1 and 4 h (Init. is used for the initial condition).

intensity is accompanied by decrease in the intensity and broadening of the peaks at diffraction angle 430 [17].

The microstructure of Inconel 718 after different modes of plasma nitriding is presented in Fig. 2, where the surface nitrided layer is separated from the substrate by a well manifested line. By the data of the XRD this layer is represented by CrN nitride. Formation of such a layer has been observed in [6, 13, 14, 16, 17].

The appearance of a CrN layer is associated with the high rate of the sputtering – redeposition process and rapid reaction between nitrogen and chromium. This does not permit nitrogen to penetrate deeply into the surface layer, and the diffusion layer is very narrow [17]. For this reason, the specimens behave like coated ones rather than like nitrided ones. For example, it can be seen in Fig. 2 that the nitride layer is as if separated from the surface of the substrate. Such an effect has been observed in plasma nitriding of stainless steel 316L [19]. However, when the duration and the temperature of the process are increased, the effect is suppressed and the adhesion between the nitride layer and the substrate increases.

Table 1 presents the roughness of the surface and the thickness of nitride layers on specimens. When the parameters of the process grow, the roughness of the surface increases. Ion bombardment and rapid sputtering, which intensify with growth in the parameters of the process, cause degradation of the surface texture [17]. Another important effect is thickening of the layer upon growth of the time and temperature of the treatment. It is shown in [14, 15] that the thickness of the layer is maximum at critical values of the temperature and time of the process, after which the thickness of the layer decreases. However, the authors of [16] report continuous growth of the thickness of the layer. Our data agree with the results of [16]. On the other hand, the duration of plasma nitriding in [14, 15] was great. We see that long-term plasma nitriding can result in thinning of the nitride layer, while penetration of nitrogen into the substrate may limit the growth of the layer, as it is reported in [17].
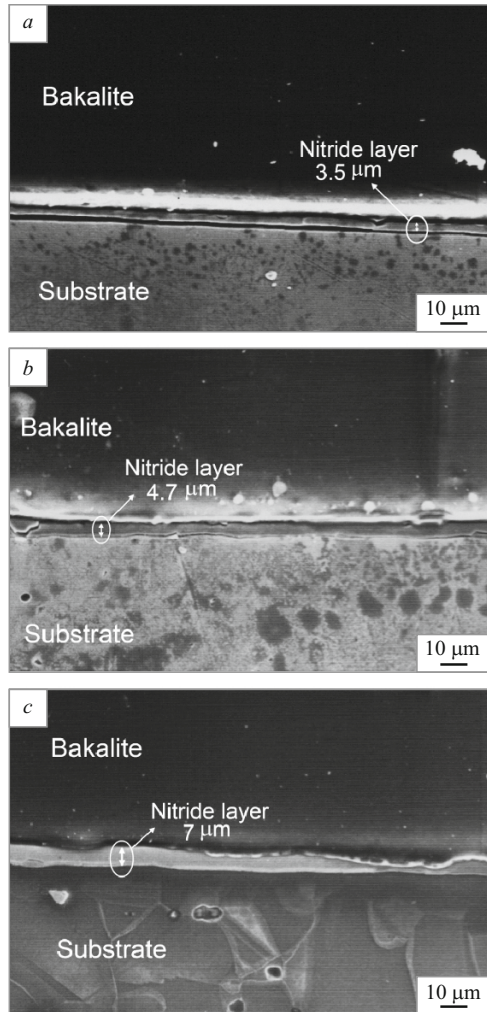
Fig. 2. Microstructure of specimens of Inconel 718 in cross section after plasma nitriding at 400°C for 1 h (*a*), at 600°C for 1 h (*b*), and at 600°C for 4 h (*c*) (scanning electron microscopy).
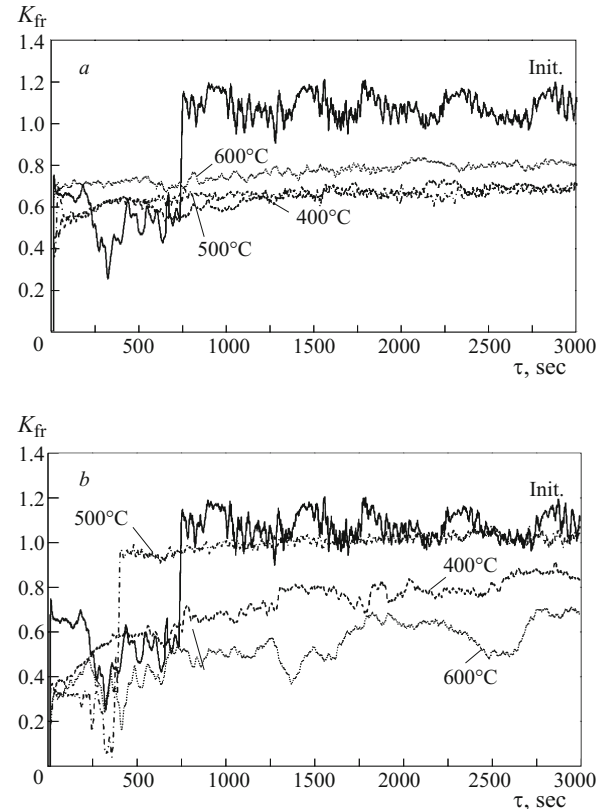

Fig. 3. Variation of the friction coefficient in friction tests of Inconel 718 in the initial condition (Init.) and after plasma nitriding for 1 h (*a*) and 4 h (*b*) at 400, 500, and 600°C.

The data of Table 1 show that prolongation of the process is more effective for thickening of the layer than increase of the temperature.

Table 2 presents the values of the elastic modulus and of the micro- and nanohardness of surface layers. The micro-hardness grows with the parameters of the process. The data for specimens 400-1 and 600-4 with the lowest and highest values of the time and temperature of nitriding show that the microhardness increases by a factor of 2.3 and 5.5, respectively, as compared to the untreated condition. The same tendency has been observed in [14, [17]. The data on the nanohardness and on the elastic modulus obey the same tendency, i.e., both parameters increase with the time and temperature of the process. The elastic modulus of the CrN layer

TABLE 1. Surface Roughness *Ra* and Average Thickness of Nitride Layer in Alloy Inconel 718 after Plasma Nitriding

Specimen	Mode of nitriding	Ra, μm	h_{av}, μm
400-1	400°C, 1 h	0.050 − 0.550	3.5 ± 0.20
400-4	400°C, 4 h	0.122 − 0.126	5.4 ± 0.40
500-1	500°C, 1 h	0.062 − 0.065	4.0 ± 0.50
500-4	500°C, 4 h	0.134 − 0.139	6.2 ± 0.30
600-1	600°C, 1 h	0.086 − 0.900	4.7 ± 0.50
600-4	600°C, 4 h	0.175 − 0.178	7.0 ± 0.60
Initial	–	0.030 − 0.035	–

TABLE 2. Hardness and Elastic Modulus of Alloy Inconel 718 after Plasma Nitriding

Specimen	Mode of nitriding	$HV_{0.01}$, kgf/mm²	HV_s, GPa	E, GPa
400-1	400°C, 1 h	1142.20	6.76	231.99
400-4	400°C, 4 h	1574.70	9.09	307.46
500-1	500°C, 1 h	1353.10	8.11	278.38
500-4	500°C, 4 h	2411.30	12.10	361.93
600-1	600°C, 1 h	2302.30	10.59	339.56
600-4	600°C, 4 h	2655.60	14.26	374.45
Initial	—	481.90	4.78	220.84

Notations: $HV_{0.01}$) microhardness; HV_s) nanohardness of the surface; E) elastic modulus of the surface.
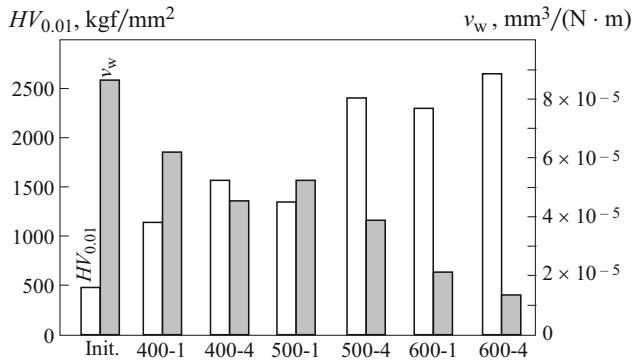
Fig. 4. Microhardness $HV_{0.01}$ and wear rate vw of specimens of Inconel 718 in the initial condition and after plasma nitriding for 1 h and 4 h at 400, 500, and 600°C.

deposited by plasma nitriding ranges from 232 to 374 GPa. This agrees with the data of [20 – 22], where the layers of chromium nitride were obtained by other methods. The values of the nanohardness and of the elastic modulus are the highest after 4-h nitriding at 600°C. Continuous growth of these properties is explainable by the microstructure of the layer. It is shown in [17, 18] that a plasma-nitrided layer of CrN has a columnar structure with pores. The surface of the specimen is fully covered with a layer with a columnar structure after a durable nitriding and elevation of the temperature.

The results of the friction tests of alloy Inconel 718 are presented in Fig. 3. It can be seen that the nitriding reduces the friction coefficient, and the curves of variation of the friction coefficient during testing are quite smooth. The behavior of the not nitrided specimen in the friction test is comparable to the data of [6, 17], where the form of the variation of the

friction coefficient in the tests is wavy. In our study the friction coefficient also decreased with growth in the hardness due to nitriding. The specimen with the highest hardness and elastic modulus after the treatment at 600°C for 4 h has the lowest friction coefficient. The plots reflect the oscillating behavior of the friction coefficient. This is explainable by detachment and separation of the nitride layer from the surface under the sliding process, which produces an abrasive effect. It should also be noted that the specimen treated for 4 h behaves in a special manner. It can be seen from Fig. 3b that in this case the oscillations are more manifested than in the other specimens. Presumably, this is a result of the strong roughness of the surface after the 4-h treatment.

Figure 4 presents the values of the microhardness and of the wear rate obtained after different modes of nitriding. The untreated specimens exhibit the highest wear rate that decreases upon growth in the time and temperature of the nitriding process. Depending on the growth in the surface hardness, the contact area deceases, which results in decrease in the friction coefficient. The wear resistance increases with growth of the surface hardness; the wear rate and the microhardness obey about an inverse dependence.

Figure 5 presents the surface of wear tracks on the specimens. The untreated specimen is worn considerably due to the strong plastic deformation (Fig. 5a). Nitriding reduces the width of the wear tracks in accordance with growth in the wear resistance.

The CrN layer detaches locally from the substrate material during sliding. Such behavior has also been observed in [18] and explained by local contact stresses between the specimen and the rider. Local detachment and separation of the hard nitride layer hinders smooth sliding in the friction
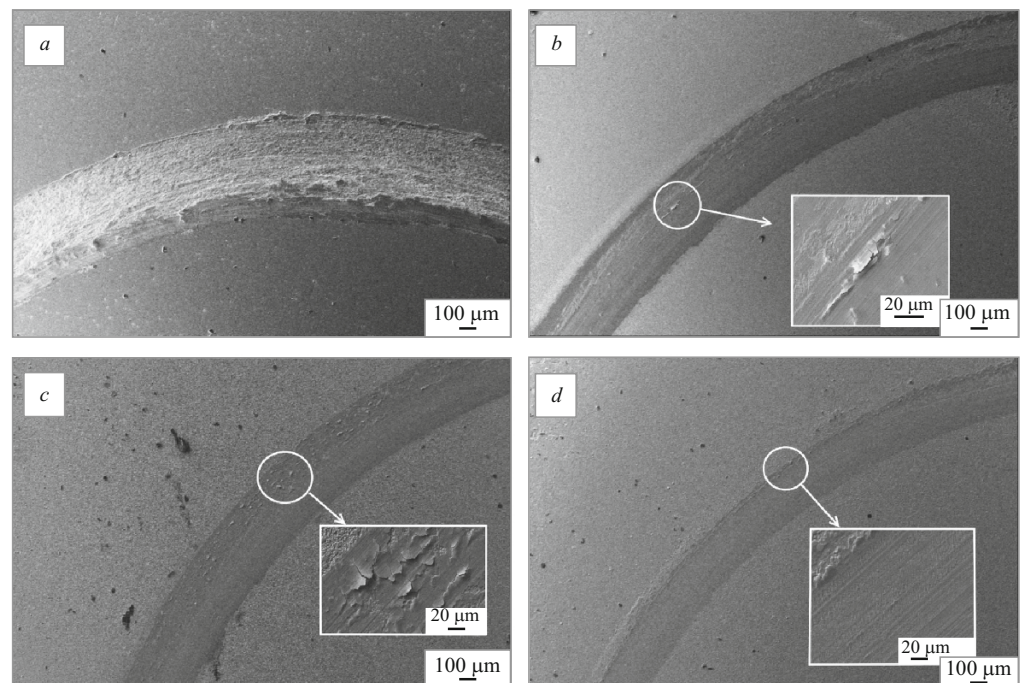

Fig. 5. Sliding tracks in wear tests of Inconel 718 in the initial condition (*a*) and after 4-h plasma nitriding at 400°C (*b*), 500°C (*c*) and 600°C (*d*) (scanning electron microscopy).

pair. In addition, the detachment depends on the special features of the plasma-nitrided CrN layer. It looks like a coating rather than like a diffusion layer. This can be observed in Fig. 2*a*, where the nitride layer has partially separated from the substrate material, i.e., the adhesion of the nitride layer is too poor. Growth in the time and temperature of nitriding intensifies the adhesion and increases the thickness and the hardness of the layer (Fig. 2*b* and *c*). Separation of the layer having the form of a plate is not observed in the specimen treated at 600°C for 4 h (Fig. 5*d*). In addition, this specimen has the narrowest and smoothest wear tracks. The best wear resistance of this specimen is the result of the great thickness of the nitride layer, high hardness and high elastic modulus. The fracture mechanism of alloy Inconel 718 after plasma nitriding is discussed in [6, 17, 18]. In [17], it is assumed that flake-like debris form in the wear process after nitriding. In [6], the wear mechanism is described as adhesion wear due to sticking. In the present work we assume that the main mechanism is abrasive wear due to detachment of the nitride layer under sliding. The concept is confirmed by the variation of the friction coefficient (Fig. 3) and by the appearance of wear tracks (Fig. 5). However, the behavior of specimen 600-4 differs. It looks like a specimen tested for adhesion wear, because the sliding track in Fig. 5*d* is smooth, and the nitride layer is not detached. On the whole, the tribological studies have shown that the wear behavior of Inconel 718 after plasma nitriding varies from an intense one to abrasive and adhesive ones.

CONCLUSIONS

1. Plasma nitriding of alloy Inconel 718 produces a thin well manifested layer of CrN nitride.

2. The thickness, the micro- and nanohardness, the elastic modulus of the layer and the surface roughness increase with the duration and temperature of the nitriding process. From the standpoint of changes in the properties of the layer, growth in the duration of the treatment is more efficient.

3. The friction coefficient of the alloy after plasma nitriding is the lowest when the latter is conducted at 600°C for 4 h, when the hardness, the elastic modulus and the thickness of the nitride layer are the highest.

4. Plasma nitriding of alloy Inconel 718 provides substantial improvement of its wear resistance; the wear mechanism depends on the parameters of the process. The highest wear resistance is obtained after 4-h plasma nitriding at 600°C.

REFERENCES

1. A. Altin, M. Nalbant, and A. Taskesen, "The effects of cutting speed on tool wear and tool life when machining Inconel 718 with ceramic tools," *Mater. Design*, **28**, 2518 – 2522 (2007).

2. A. Bhatt, H. Attia, R. Vargas, and V. Thomson, "Wear mechanisms of WC coated and uncoated tools in finish turning of Inconel 718," *Tribology Int.*, **43**, 1113 – 1121 (2010).

3. Y. Chen and Y. Liao, "Study on wear mechanisms in drilling of Inconel 718 superalloy," *J. Mater. Proc. Technol.*, **140**, 269 – 273 (2003).

4. J. Costes, Y. Guillet, G. Poulachon, and M. Dessoly, "Tool-life and wear mechanisms of CBN tools in machining of Inconel 718," *Int. J. Mach. Tools Manuf.*, **47**, 1081 – 1087 (2007).

5. W. F. Smith, *Structure and Properties of Engineering Alloys* (1993).

6. V. Singh and E. I. Meletis, "Synthesis, characterization and properties of intensified plasma-assisted nitrided superalloy Inconel 718," *Surf. Coat. Technol.*, **201**, 1093 – 1101 (2006).

7. A. Houghton, R. Lewis, U. Olofsson, and J. Sundh, "Characterising and reducing seizure wear of inconel and incoloy superalloys in a sliding contact," *Wear*, **271**, 1671 – 1680 (2011).

8. B. Edenhofer, "Physical and metallurgical aspects of ionitriding," *Heat Treat. Met.*, Pt. 1, 23 – 28 (1974).

9. A. Alsaran and A. Celik, "Structural characterization of ion-nitrided AISI 5140 low-alloy steel," *Mater. Charact.*, **47**, 207 – 213 (2001).

10. A. Çelik and S. Karadeniz, "Improvement of the fatigue strength of AISI 4140 steel by an ion nitriding process," *Surf. Coat. Technol.*, **72**, 169 – 173 (1995).

11. A. Rizk and D. McCulloch, "Plasma nitriding of Inconel 625," *Surf. Technol.*, **9**, 303 – 315 (1979).

12. C. Leroy, T. Czerwiec, C. Gabet, et al., "Plasma assisted nitriding of Inconel 690," *Surf. Coat. Technol.*, **142**, 241 – 247 (2001).

13. T. Borowski, A. Brojanowska, M. Kost, et al., "Modifying the properties of the Inconel 625 nickel alloy by glow discharge assisted nitriding," *Vacuum*, **83**, 1489 – 1493 (2009).

14. Y. Sun, "Kinetics of layer growth during plasma nitriding of nickel based alloy Inconel 600," *J. Alloys Comp.*, **351**, 241 – 247 (2003).

15. F. Kahraman and S. Karadeniz, "Characterization and wear behavior of plasma nitrided nickel based dental alloy," *Plasma Chem. Plasma Proc.*, **31**, 595 – 604 (2011).

16. C. Sudha, R. Anand, Paul V. Thomas, et al., "Nitriding kinetics of Inconel 600," *Surf. Coat. Technol.*, **226**, 92 – 99 (2013).

17. P. Aw, A. Batchelor, and N. Loh, "Structure and tribological properties of plasma nitrided surface films on Inconel 718," *Surf. Coat. Technol.*, **89**, 70 – 76 (1997).

18. P. Aw, A. Batchelor, and N. Loh, "Failure mechanisms of plasma nitrided Inconel 718 film," *Wear*, **208**, 226 – 236 (1997).

19. F. Yildiz and A. Alsaran, "Multi-pass scratch test behavior of modified layer formed during plasma nitriding," *Tribology Int.*, **43**, 1472 – 1478 (2010).

20. L. Cunha, M. Andritschky, K. Pischow, and Z. Wang, "Microstructure of CrN coatings produced by PVD technique," *Thin Solid Films*, **355**, 465 – 471 (1999).

21. H. Ichimura and I. Ando, "Mechanical properties of arc-evaporated CrN coatings. Part I. Nanoindentation hardness and elastic modulus," *Surf. Coat. Technol.*, **145**, 88 – 93 (2001).

22. J. A. Sue, A. J. Perry, and J. Vetter, "Young's modulus and stress of CrN deposited by cathodic vacuum arc evaporation," *Surf. Coat. Technol.*, **68**, 126 – 130 (1994).